Latin American Journal of Solids and Structures
www.lajss.org

Damage evaluation and failure mechanism analysis of steel tube confined reinforced-concrete columns by acoustic emission technology

Abstract

As a new kind of composite structures and its advantages, the using of steel tube confined reinforced concrete (STCRC) columns have received increasing attention in civil engineering. Acoustic emission (AE) technique is applied to monitor the damage process of STCRC columns during an uniaxial compression test. The aim of this study is to investigate the damage evaluation and failure mechanisms of the STCRC columns from the perspective of microscopic damage. Typical AE parameters are extracted to quantify different damage condition and identify the critical point. Peak-frequency analysis classify the damage signal into groups, representing different AE generation mechanisms. Extended AE features, such as the RA value and the average frequency are calculated to discriminate the cracking modes of core concrete. The probability based Gaussian mixture model (GMM) are proposed for unsupervised damage pattern recognition. All presented AE results are good in accordance with the observed experimental outcomes. The AE technology enabled evaluating the damage condition, identifying critical point, disclosing the failure mechanism, and classifying damage modes for steel confined RC columns effectively.

Keywords

steel tube confined RC column, acoustic emission, damage evaluation and classification, failure mechanism, critical warning

Fangzhu Du[a,b]
Shengshan Pan[a*]
Dongsheng Li[a,b]

[a] School of Civil Engineering, Dalian University of Technology, Dalian 116024, China. E-mail: fangzhudu@mail.dlut.edu.cn, pssbu@dlut.edu.cn, lidongsheng@dlut.edu.cn

[b] State Key Laboratory of Coastal and Offshore Engineering, Dalian University of Technology,Dalian 116024, China.

*Corresponding author

http://dx.doi.org/10.1590/1679-78255339

Received: October 25, 2018
In Revised Form: October 26, 2018
Accepted: October 26, 2018
Available online: October 29, 2018

1 INTRODUCTION

Steel/concrete composite structure has been widely applied in high-rise buildings, long-span bridges and underground structures. Therein, concrete-filled steel tube (CFST) columns is one of the preferred components of these large-scale projects because of high bearing capacity, good seismic performance and excellent ductility (Sakino et al., 2004; Schnabl and Planinc, 2017). However, some researchers (Ding et al., 2011) reported that the confinement effect does not occur during the elastic stage when Poisson's ratio of steel is higher than that of core concrete. The premature buckling of steel tubes under biaxial stress will further decrease the ductility of CFST columns. Furthermore, the connection between the CFST columns and RC beam is quite complicated, which then lead to great difficulty in design and construction. In order to overcome these problems, some scholars (Riyad and Rafael, 1998; Liu et al., 2009) have put forward the improved structure form called steel tube confined reinforced concrete (STCRC) columns. The most prominent feature of STCRC column is that the outside steel tube was cut off at both ends. Therefore, the axial load is directly applied on the core concrete, while the steel tube is mainly used for lateral restraint so that core concrete could be confined more effectively. Zhou et al. (2008) and Wang et. al (2017) thoroughly investigated the mechanical and performance of the STCRC columns, and illustrated that the steel tube in STCRC column shows a better confinement effect and seismic behaviour than that of CFST column. Different from the traditional RC structure, the STCRC column possesses a highly complex and sheltered failure mechanism by combining steel tubes, concrete, and steel rebar, and the damage process of the wrapped core concrete can not be observed directly. Thus, developing a continuous monitoring and non-destructive evaluation method to assess the damage deterioration in STCRC structure is in great demand.

(cc) BY

Structural health monitoring (SHM) started from 1980s, and developed greatly in civil engineering in recent years. SHM can detect, locate, and quantify structural damages based on measurement and analysis of data from sensors, that help us know the safety and amenity of structures, has emerged as a promising technology for instantaneous assessment of damages and deterioration in structures (Yang et al., 2008; Liu et al., 2012; Döhler et al., 2014). Acoustic emission (AE) is a non-destructive testing (NDT) technique and can provide reliable and real-time information on the condition of the structure, has been extensively explored in civil engineering for SHM and damage evaluation. This technique utilizes the detection of transient elastic waves caused by plastic deformation or cracks propagation during the increasing load or material deterioration. Piezoelectric AE transducers can detect the micro-vibration on the surface of material and convert it into a usable electric signal, called AE signal (Sengupta et al., 2015). AE signal contains useful information on the material damages, the location, mechanism, and severity of the AE source can be assessed by analysis of the resultant waveform. AE is sensitive to small damages, and it not only can monitor the damage state of the sensor site, but also can monitoring certain areas where excited stress wave are readily accessible, without having to affect the integrity of structures (Philippidis and Assimakopoulou, 2008). Given its unique superiorities, numerous researchers have shown that the AE monitoring technique could be applied to damage evaluation for civil engineering structures, such as concrete structures (Farhidzadeh et al., 2013a), composite structures (Ma and Li, 2017), and huge bridges(Nair and Cai, 2010), and so on.

To the author's best knowledge, previous studies mostly focused on the mechanical behaviour, seismic behaviour, and constitutive model for steel tube confined RC structure, but the cognition of its health monitoring and damage mechanism has not been comprehensively illustrated. Du et al. (2018) reported the AE monitoring and evaluating for the steel confined RC columns under seismic loading, however, the interior failure mechanisms and fracture modes was not touched. This study concentrate on the continuous AE monitoring and evaluation for STCRC columns during axial compression test. Typical AE parameters are extracted for damage tracing and condition assessment, several promising methods are applied to further analyze the cracking mechanism and classification. Pursuant to the Japanese code JCMS-III B5706 (2003), the relationship between RA value (rise time/amplitude) and average frequency (counts/ duration) can be used for the crack classification in concrete structures. For most case of materials from initial load to destruction, tensile cracks are developed at the initial stage of loading, while shear cracks gradually dominate later (Aggelis, 2011; Ohno and Ohtsu, 2010). Therefore, the classification of cracks can contribute to the determination of failure pattern and critical warning. However, a quantified criterion on the proportion of these two parameters (RA and AF) has not been confirmed yet. Considering the fact that the obtained AE signals are affected by many factors, such as the type of AE sources, the resonate frequency of sensors, and the propagation path from the AE source to sensor, et al. Recently, a popular probabilistic method called Gaussian mixture model (GMM) has been proposed for concrete crack classification (Farhidzadeh et al., 2015; Farhidzadeh et al., 2013b). The GMM algorithm overcome some deficiencies of conventional crack classification method, and the component densities of GMM can model an underlying set of hidden classes (Farhidzadeh et al., 2013b; Wang et al., 2018).

The present research aim at employ the prevailing AE technique to monitor the damage process of the steel tube confined RC columns under compressive loading, so as to reveal its damage evolution and failure mechanisms from the perspective of micro scope. 1) Typical AE parameters, such as energy and rise time, are extracted for damage evolution analysis. 2) The integrated analysis of loading process, cumulative energy, and peak frequency are conducted to reveal failure mechanisms and provide critical warning. 3) The correlation analysis of RA value and average frequency are incorporated with the peculiar Gaussian mixture model (GMM), to discriminate the shear and tensile cracks from the probabilistic view.

2 EXPERIMENTAL PROCEDURE

2.1 Specimen preparation

A total of six STCRC columns were divided into three test groups, with different steel thickness and concrete strength. The height of each column was 510 mm, and the inner diameter was 170 mm, as shown in Figure 1 and Figure 2. The manufacture and test of the specimens were based on the *Chinese Code for the Design of Concrete Structures* (*GB50010-2010*). To avoid the steel tube bearing the axial load directly, two loops with 10 mm widths were cut off at 40 mm from both ends. The basic information of test specimens are listed in Table 1. For conciseness, C-1-60, C-2-60, C-2-80 are used to denote the three test group in the fowling chapter.

Table 1: *Basic Information of Test Specimen.*

Type	Number of specimen	Concrete strength	Steel tube Thickness (mm)	Radius-thickness ratio (D_s/t_s)
C-1-60	2	C40	1	172
C-2-60	2	C60	2	87
C-2-80	2	C80	2	87

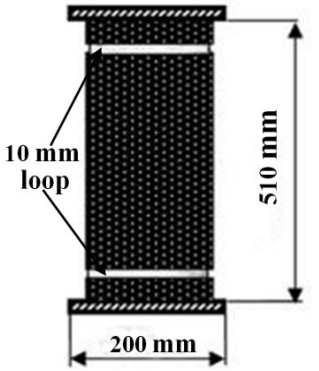

Figure 1: *Schematic diagram of test specimens.*



Figure 2: *Photo of test specimen.*

2.2 Material properties

The customized steel tube used in the experiment was Steel Q235 with the thickness of 1 mm or 2 mm. The mechanical properties of the steel tube were obtained from a standard tensile test of prepared coupons, according to *Chinese Code for Metallic materials— Tensile testing at ambient temperature* (*GB/T228-2002*). Detailed steel properties are shown in Table 2. This experiment employed two types of commercial concrete, the nominal C60 and C80, manufactured by *Dalian JINHE Concrete Mixing Plant*. The standard cube specimens were cured and tested in accordance with *Chinese Code for Test and Evaluation of Concrete Strength* (*GB50107-2010*). The tested average concrete compressive strength of C60 and C80 was 68.7 MPa and 81.1 MPa, respectively. The adopted longitudinal rebar was 6Φ12 and its reinforcement ratio was 2.98%. The allocation of stirrup was Φ6@100 and the corresponding volume ratio was 1.13%.

Table 2: *Mechanical properties of steel tube.*

Thickness (mm)	E-modulus (GPa)	yield strength (MPa)	Tensile strength (MPa)
1	210	188	330
2	204	192	345

2.3 Experimental setup

The specimens were tested on a 10000 kN hydraulic testing machine made by *Beijing Fluid Control System (FCS) Corp*. Two displacement meters were set on the loading station to monitor the axial displacement, strain gages were attached to the middle surface of the tube to measure the axial and circular strain, and a calibrated load cell was used to record the axial pressure. The loading protocol was applied by displacement control, maintained at a loading rate of 0.5 mm/min.

A two-channel MISTRAS 2001 data acquisition system from the *American Physical Acoustics Corporation* was used to record AE signals during the entire test process. Two R15a resonant AE transducers were symmetrically placed in the middle of the specimen, using Vaseline as coupling agent, and connected to the AE monitor system via preamplifier, see in Figure 3. Prior to starting the test, the pencil-lead break procedure was performed to ensure that two AE transducers were in good working condition. To guarantee the rationality of the collected data, the basic parameters of AE monitor system were set as follows: the main amplifier gain was set at 20 dB, preamplifier gain was 40 dB, sample rate was 3 MHz and the threshold of the was fixed at 40 dB throughout the monitoring process to avoid surrounding disturbance. Figure 3 provides the schematic of test equipment and AE system.

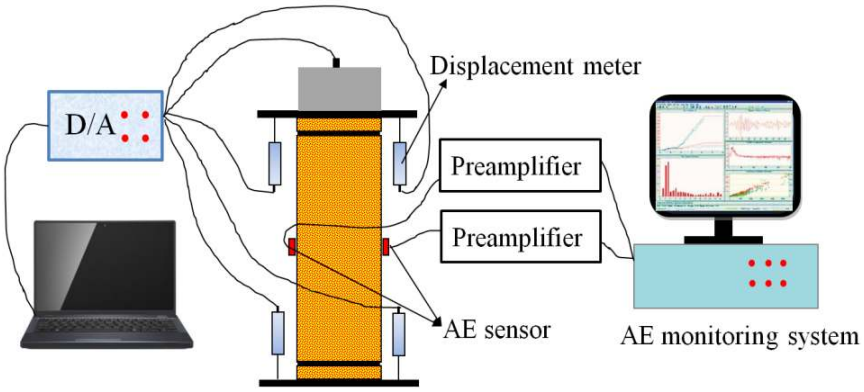

Figure 3: *Experimental schematic and AE system.*

3 ANALYTICAL METHODOLOGY

3.1 RA Value and Average Frequency (AF)

The *Japanese Construction and Material Standard (JCMS-III B5706, 2003*) proposed a technique to monitor the crack propagation in concrete structures based on two AE parameters, namely RA value and average frequency (AF). RA value is defined as the ratio of rise time to amplitude, while AF is defined as the AE counts divided by the duration of the signal. The formula of these two parameters are presented in the following equations:

$$\text{RA} = \text{Rise time}/\text{Amplitude} \tag{1}$$

$$\text{AF} = \text{Counts}/\text{Duration} \tag{2}$$

According to previous researches (Aggelis, 2011), the type of concrete fracture can be classified as a shear failure or a tensile failure. When an AE signal has low average frequency and high RA value, it is classified as shear type crack. By contrast, a signal with high average frequency and low RA value, is classified as tensile crack, as demonstrated in Figure 4. Generally speaking, tensile cracks should be related to the progressive development of new cracks, while shear cracks can be associated with the sliding and mutual-connection of existing cracks. The crack mode can be classified by separating the flexural and shear sources based on the predefined diagonal line in Figure 4.

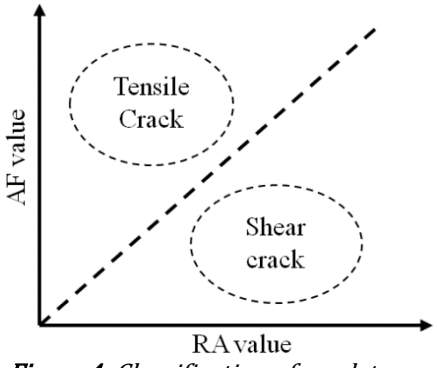

Figure 4: *Classification of crack types.*

3.2 Gaussian mixture model

Gaussian mixture model (GMM) is a popular probabilistic method and has been successfully used in many research fields. Except density estimation, the algorithm is also widely used for data-clustering. In mathematics, GMM can be represented as a weighted sum of k component Gaussian densities. For a D-dimensional feature vector x, the mixture density is defined as,

$$p(x|\lambda)=\sum_{j=1}^{k}\alpha_j N_j(x|\mu_j,C_j) \quad ;\ j=1,\cdots,k \tag{3}$$

where $\acute{a}_j$ represents the mixture weights. The mixture weights must satisfy the following constraint,

$$\sum_{j-1}^{k}\alpha_j=1;\ j=1,\cdots,k \tag{4}$$

and N_j $(x|\dot{g}_j,C_j)$ represents the D-dimensional unimodal Gaussian (Normal) distribution, corresponding density function is given by the following equation,

$$N_j(x|\mu_j,C_j)=\frac{1}{\sqrt{(2\pi)^{D/2}}|C_j|^{1/2}}\exp\left[-\frac{1}{2}\left(x-\mu_j\right)^T C_j^{-1}\left(x-\mu_j\right)\right] \tag{5}$$

where $\dot{g}_j$ is a $D\times 1$ mean vector, and C_j is a $D\times D$ covariance matrix. The GMM is parameterized by the mean vectors, covariance matrices, and mixture weights of each Gaussian distribution. These parameters can be grouped as,

$$\lambda=(\alpha_j,\mu_j,C_j)\ ;\ j=1,\cdots,k \tag{6}$$

Generally, the expectation–maximization (EM) algorithm can be used to estimate the parameters λ of the GMM (Roberts and Furui, 2000; Tagare et al., 2010). The EM algorithm is an iterative learning that maximizes the likelihood function generated by each GMM. In this study, GMM algorithm is proposed to classify a two-dimensional AE feature vector X= (RA, AF) into two clusters. Elements belong to one cluster is associated to tensile cracks, while elements belong to another cluster should be attributed to shear cracks.

4 DAMAGE EVALUATION BASED ON TYPICAL AE PARAMETERS

4.1 Damage evaluation and basic AE response

The compression test results and AE responses of all specimens are shown in Table 3, Figure 5, Figure 6, and Figure 7 provide the correlation between typical AE parameters and loading history for group C-1-60, C-2-60, and C-2-80, respectively. The red curve represents the axial load, while the blue curve represents the variation of cumulative AE energy or AE rate. The results showed that all the specimens presented the similar variation trend of AE activity. Figure 8 provides the ultimate damage pattern of each test group.

AE energy, derived from the time integral of the square of the instantaneous signal voltage $V(t)$ over the signal duration, can be related to the intensity of cracks, and the accumulation of AE energy can reflect damage severity. Figures 5(a), 6(a) and 7(a) provide the variation of cumulative AE energy and loading history during the whole damage process. With the increase of axial load, the curve of cumulative AE energy increase continuously and the damage get further intensified. There are always a noticeable knee point of slope change in cumulative energy curve, at nearly 600 s, 800 s, and 1050 s for the three test group. The cumulative AE energy increased slowly from the initial loading period and a sharp rise occurred near the ultimate load. The slowly accumulation of AE energy implies the progressive development of structural damages, while the sharp increase of AE energy means the occurrence of some major damages, and the columns are in a unstable state.

By comparison, Figures 5(b), 6(b) and 7(b) present the variation tendency of AE rate. AE rate refers to the number of AE signals collected in unit time, which can be used to measure the activity AE phenomenon. In this work, each AE rate value was calculated by every 200 AE events. During the initial stage, the stub column was in a stable state, correspondingly, the value of AE rate maintained at lower than 50 per unit. When the axial load approach 80% of the ultimate load, the distinct knee point can be observed. Subsequently, the calculated AE rate continuously increase up to about 250 per unit, which means the columns are unstable and seriously damaged.

The above observation proved that both the fluctuation of cumulative energy and AE rate can effectively reflect the damage process of STCRC columns under axial compression, and the distinct knee point can provide critical warning information for structural failure. Besides, the occurrence of distinct knee point of AE rate is always earlier than the cumulative AE energy (about 100 s early, see in Figures 5, 6 and 7), which indicates that the AE rate is more sensitive to structural damages, proved to be a prefer indicator in detecting the damage progression for STCRC structure.

It is worth noting, with the increasing of the steel tube thickness (C-1-60 and C-2-60) and concrete strength (C-2-60 and C-2-80), the loading capacity and ductility correspondingly increased, the damage pattern and AE response also show some differences. Table 3 shows that the average strength of C-2-60 is about 1.25 times of C-1-60 (with different steel tube thickness), by increasing concrete strength, the average strength of C-2-80 is about 1.45 times of C-2-60. Besides, the occurrence of knee point is delayed with the increasing of steel thickness and concrete strength (marked in Figures 5, 6 and 7), show higher deformability.

Figures 8 provides that the ultimate state of all specimens show sign of shear failure, the damage severity of group C-1-60 is higher than C-2-60 (with 2 mm steel tube), implies that the increment of steel thickness can mitigate the degree of shear failure, and the same for increase concrete strength. Whilst, the ultimate cumulative energy of the three test group show clearly increase (Table 3), that means the increment of steel tube thickness or concrete strength enhanced the STCRC columns, thus more energy are needed to deform the columns, though lighter damages occurred.

Table 3: *Basic test results of each STCRC column.*

Specimen	Number	Ultimate load (kN)	Cumulative hits	Cumulative energy (mV*is)	Maximum AE rate
C-1-60	1	1591	43133	966600	255
	2	1507	38133	823542	246
C-2-60	1	1981	40979	908203	247
	2	1876	45752	968203	241
C-2-80	1	2763	41120	1183474	239
	2	2848	43365	1083474	260

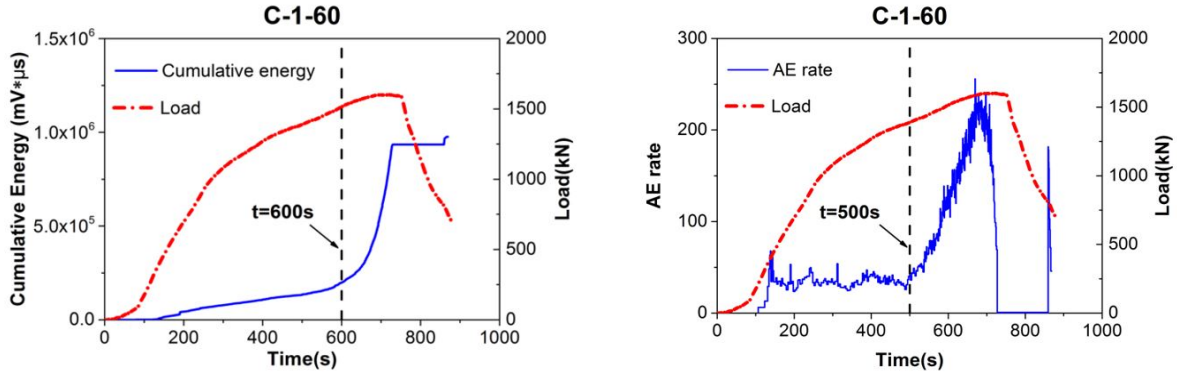

Figure 5: *Loading versus AE features for test group C-1-60, (a) cumulative AE energy versus loading history, (b) AE rate versus loading history.*

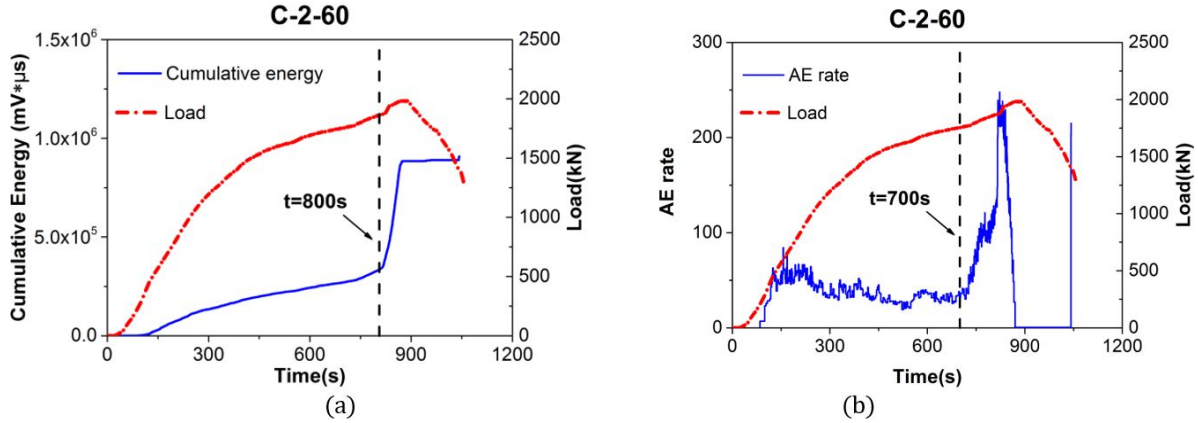

Figure 6: *Loading versus AE features for test group C-2-60, (a) cumulative AE energy versus loading history, (b) AE rate versus loading history.*

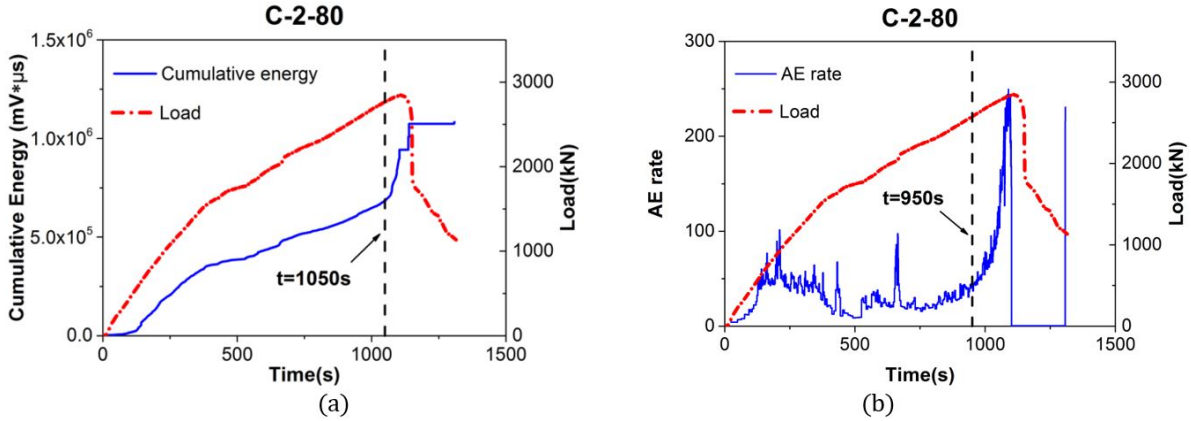

Figure 7: *Loading versus AE features for test group C-2-80, (a) cumulative AE energy versus loading history, (b) AE rate versus loading history.*



Figure 8: *Final failure modes of specimens, (a) C-1-60, (b) C-2-60, (c) C-2-80.*

4.2 Frequency based identification for damage mechanisms

Further investigation is conducted to identify the failure mechanisms of STCRC columns based on frequency distribution. In terms of the STCRC columns, the main damage modes are concrete cracking, steel/concrete interface damage, and steel deformation. Generally, peak-frequency can serve as a good AE indicator to discriminate different damage sources. According to previous literatures (Zhang et al., 2015; Zitto et al., 2015), concrete cracking usually lead to AE events with low frequency (less than 100 kHz), while damages related to steel material would contribute to AE events with a higher frequency. Figure 9, Figure 10, and Figure 11 present the distribution between AE energy and peak-frequency for each test group at different loading stages.

During the initiation of loading, the energy of high-frequency band (150 kHz–400 kHz) is greater than that of low-frequency band (Figures 9(a), 10(a) and 11(a)), the main AE sources at that stage are micro cracking of concrete. With the increasing of axial load, the proportion of AE energy in low-frequency band continuously increase, the crack propagation of core concrete is constrained, meanwhile, steel tube is gradually deformed and yielded. When reached the peak load, the energy of low-frequency band is much greater and dominated (Figures 9(b), 10(b) and 11(b)), during that time, the steel tube is severely buckled, and can not provide effective confinement, the damage of concrete increased significantly along with low-frequency signal and a huge of energy released. As a consequence, the low-frequency (<150 kHz) signals can be considered as the damages caused by concrete cracking, while the AE events with higher peak-frequency (150 kHz–400 kHz) are attributed to the interface damages and steel deformation.

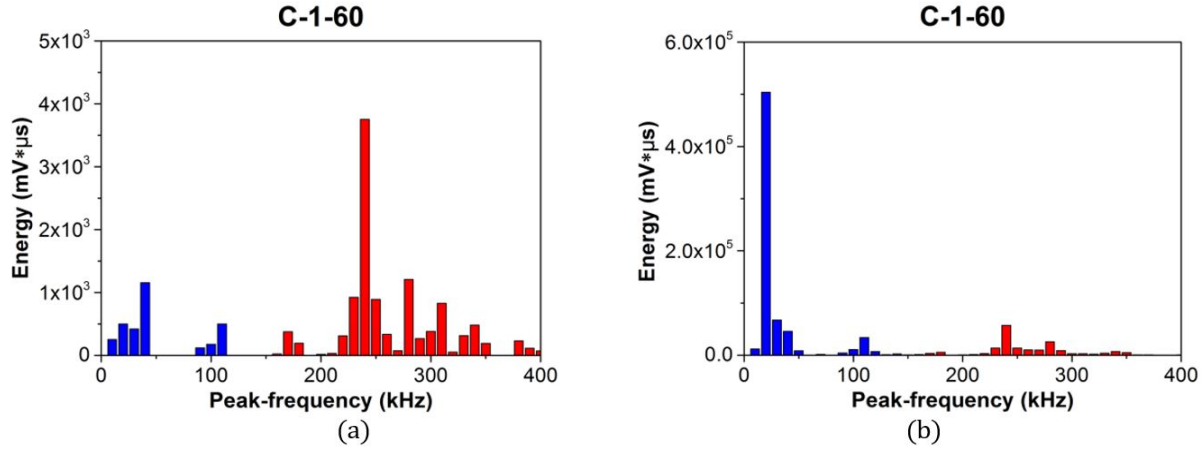

Figure 9: *Distribution between AE energy and peak-frequency for group C-1-60, (a) 30% ultimate load, (b) 100% ultimate load.*

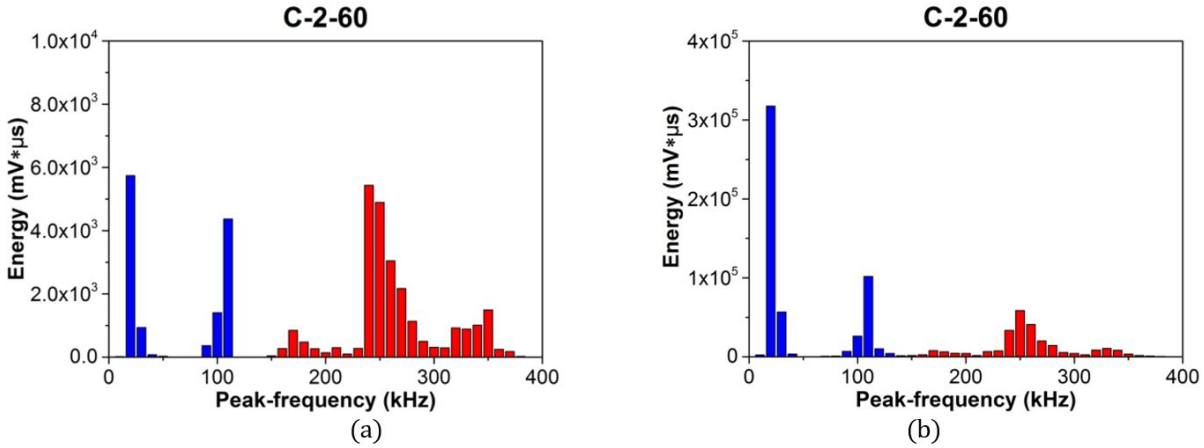

Figure 10: *Distribution between AE energy and peak-frequency for group C-2-60, (a) 30% ultimate load, (b) 100% ultimate load.*

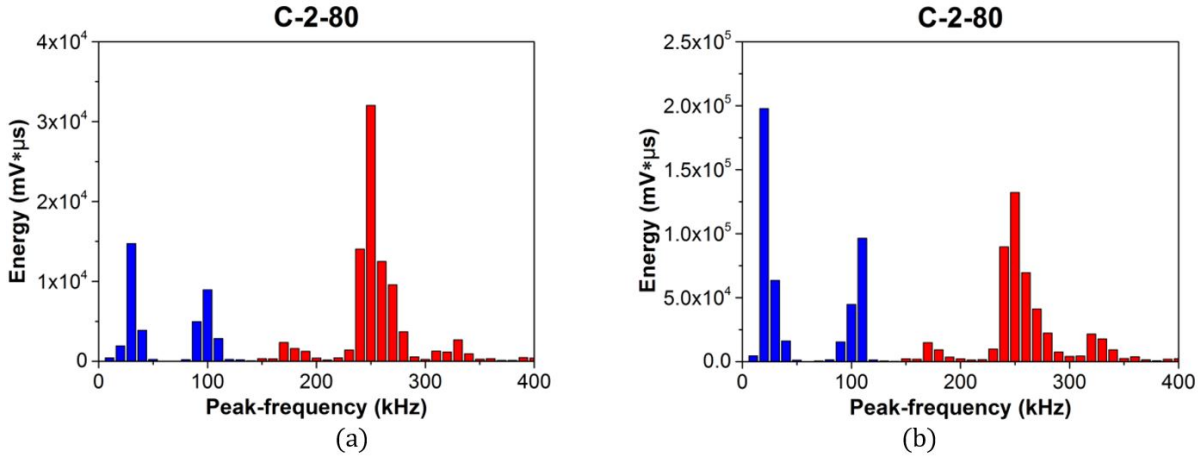

Figure 11: *Distribution between AE energy and peak-frequency for group C-2-80, (a) 30% ultimate load, (b) 100% ultimate load.*

Figure 12 presented the cumulative energy curve of two frequency bands for each test group. HP denotes high-frequency band, and LP denotes low-frequency band. With the increment of load, the energy of both two frequency bands grows continuously, but the low-frequency band increased faster. Prior to the peak load, the curve of low-frequency band increased significantly, while just a moderate rising trend appear on the curve of high-frequency band. These distinct knee points are well consistent with the knee point discussed in section 4.1, thus, the integration analysis of these proposed AE indicators can provide better early warning information for critical structural catastrophe.

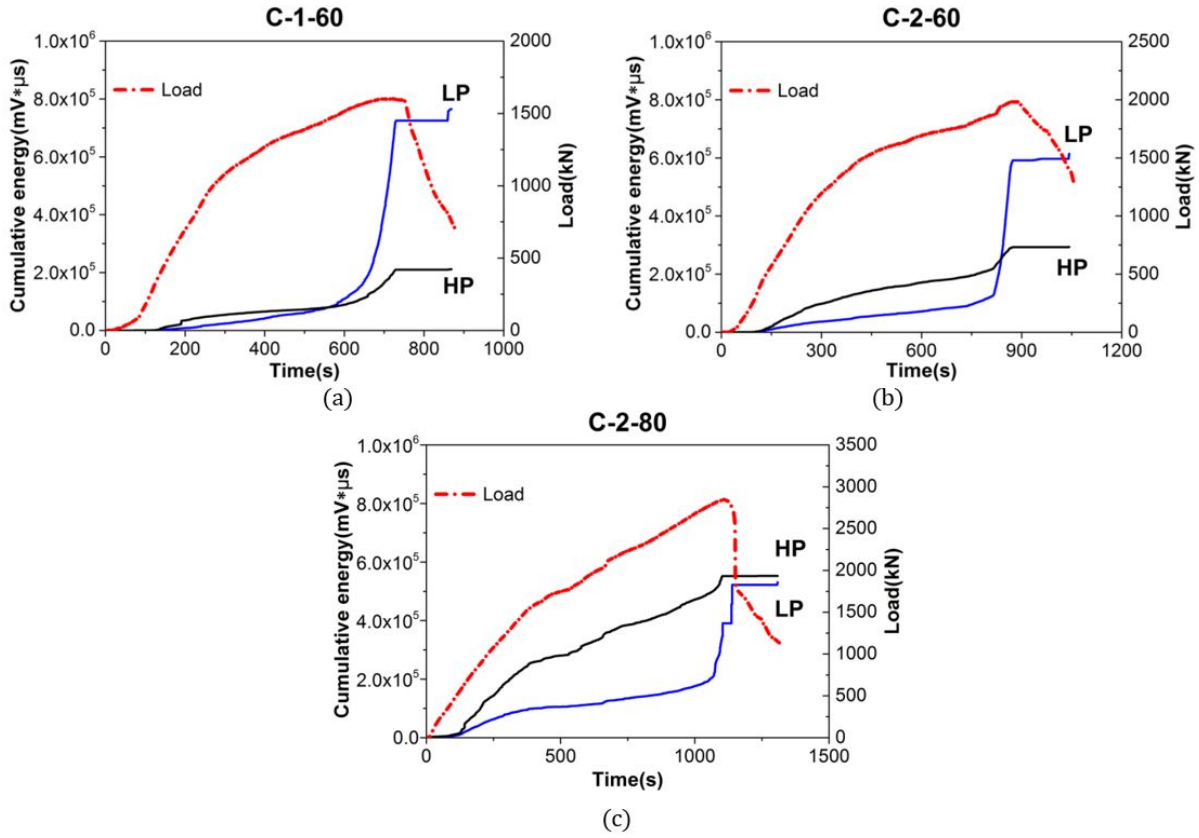

Figure 12: *Loading history versus cumulative energy of two frequency bands, (a) Group C-1-60, (b) Group C-2-60, (c) Group C-2-80.*

5 CRACK CLASSIFICATION BASED ON GMM ALGORITHM

In above section, the damage mechanisms of STCRC columns are preliminarily identified through the correlation analysis between cumulative energy and peak frequency. Further investigation on failure mechanisms are perform by RA−AF and GMM method from the perspective of the fracture modes. Tensile cracks lead to AE signals with higher average frequency and lower RA values, on the contrary, shear cracks generate signals with higher RA value and low frequency (Aggelis, 2011). Therefore, the fracture modes of STCRC columns can be determined by the RA and AF values of the AE signals. Considering that the method is fit for crack classification of concrete damages (Ohno and Ohtsu, 2010), thus only the AE events in low-frequency band (0-150kHz) are used for RA−AF crack classification.

According to Equations 1 and 2, the two features are extracted from each qualified AE signal. In this research, it is proposed to consider the dimensions of RA and AF to be μ s/dB and kHz, respectively. Then, the data set X= (RA, AF) is constructed using the two calculated features. Determination of the ratio between RA value and average frequency is important to clarify the mechanisms of cracks formation. However, there has been not a defined criterion on the proportion of the RA value and average frequency, because of numerous uncertainty factors. Cracks are classified by manually drawing a straight line in conventional crack classification, as shown in Figure 4. The Gaussian mixture model (GMM) can be used to extract the hidden feature from the complex data model, under the consideration of some uncertainty effects. Note worthily, we input data set X= (RA, AF) to the established GM model, and construct clusters by running the GMM algorithm. Figure 13 presents the classification results of three representative specimens. Blue dots represent the cluster of tensile cracks, while red dots represent the cluster of shear cracks. The results of the all specimens are remarkably similar.

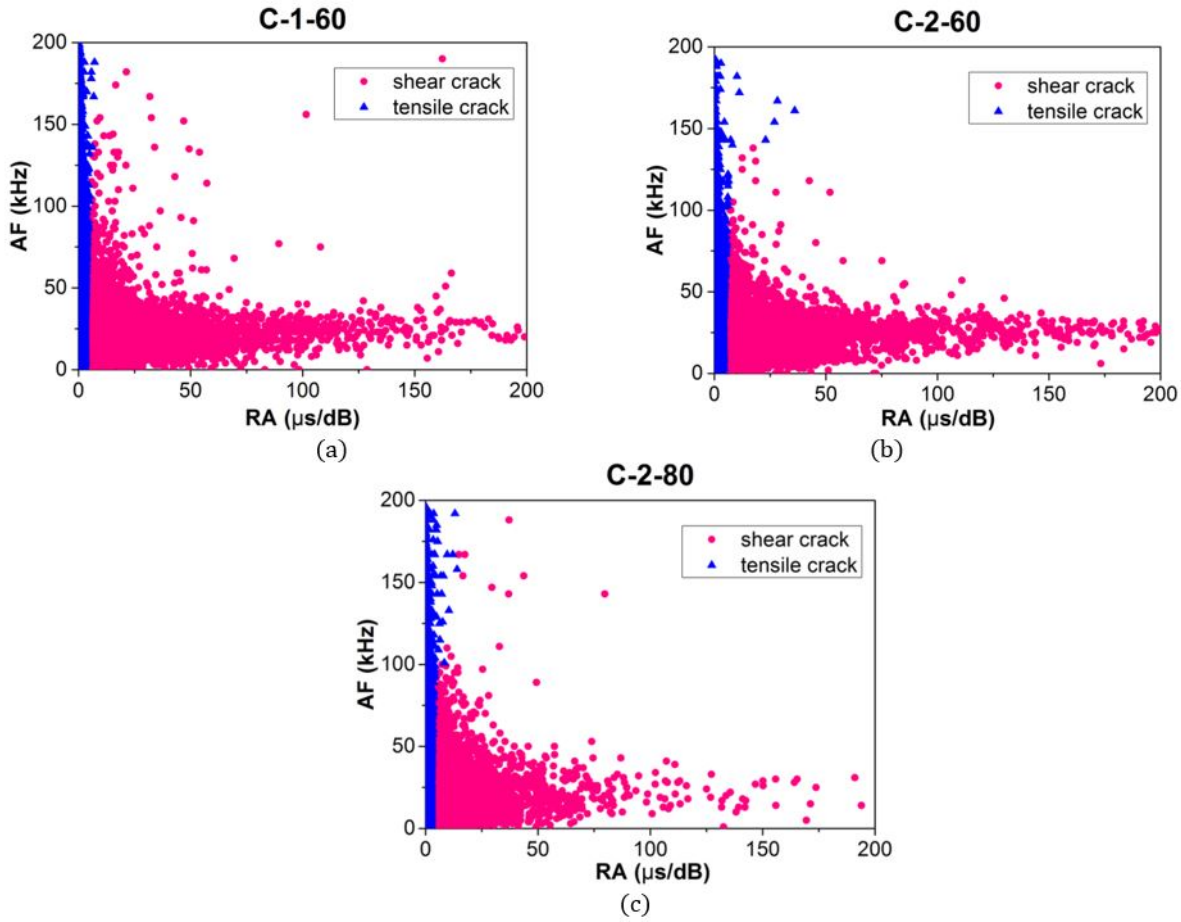

Figure 13: *Crack classification results by using GMM algorithm, (a) Group C-1-60, (b) Group C-2-60, (c) Group C-2-80.*

Figure14 shows the crack development of representative test group C-2-60 under different loading conditions. The number of shear cracks increase gradually through the loading process and become much more significant when reached the ultimate load. Figure 15, Figure 16, and Figure 17 present the fluctuation of cumulative AE energy and signal number for each class during the whole loading process. The number of shear cluster is always less than that of tensile cluster, and a significant increase of two clusters is observed before final catastrophe. Prior to the peak load, the cumulative energy of the shear cluster increased significantly, and far exceed that of tensile cluster. This result indicates that the major source of energy is the shear cracks when the final destruction occurred.

Actually, the presented AE results are well consistent with the actual experimental situation. Concrete cracked under tensile stress, and then mutual connection, resulting in the nucleation of shear cracks. Shear crack is the chief culprit that devastating the integrity of core concrete, and lead into the deterioration of bearing capacity. During the damage process, the confinement effect providing by steel tube restrain the lateral deformation (tensile crack) of core concrete, thereby the propagation of shear crack is postponed fundamentally. As a result, the potential bearing capacity of the proposed STCRC columns are fully utilized. Through the above analysis, this method has proved to be capable of well identify the fracture modes and damage mechanisms of core concrete. It is also possible to monitor the damage evolution of a real structure during whole service period, detecting the damage state and preventing structural failure.

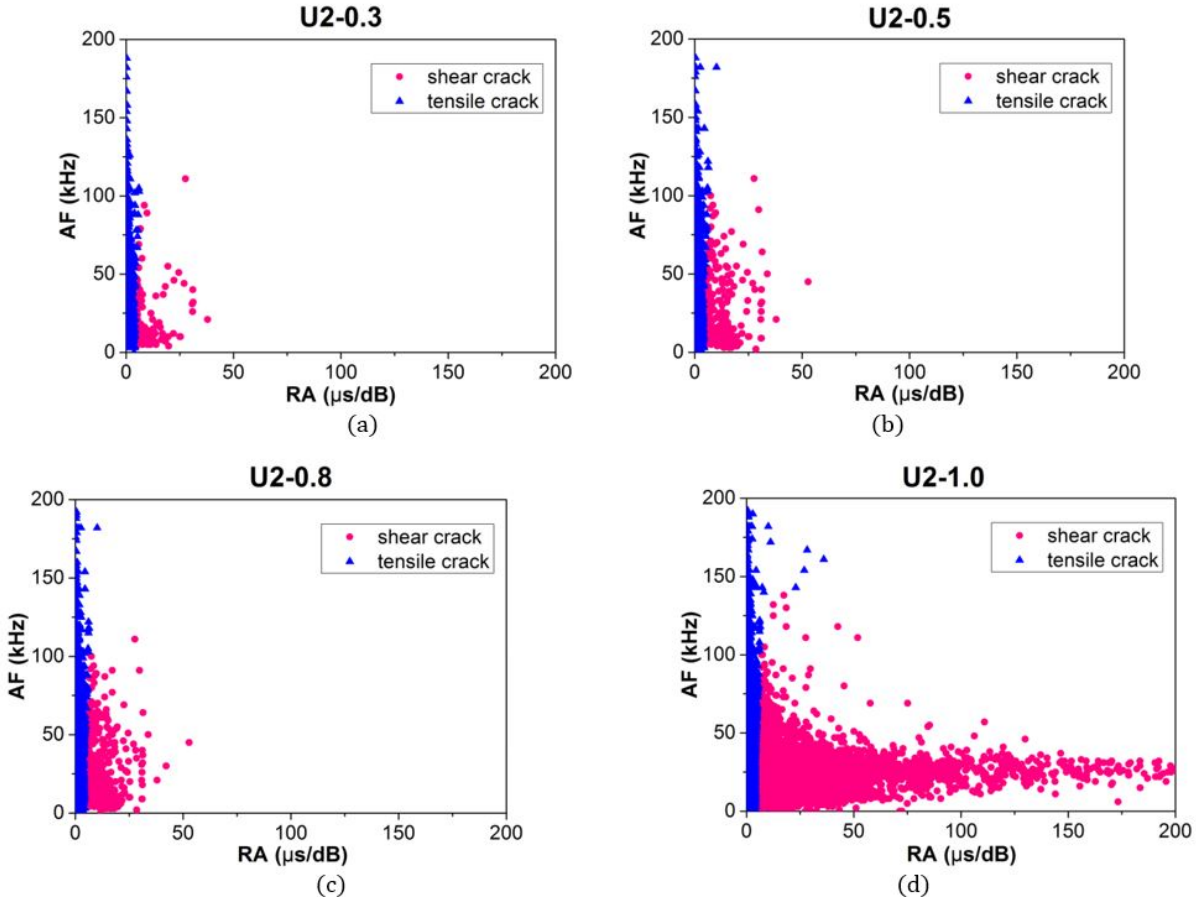

Figure 14: *Concrete cracks evolution during different loading condition for C-2-60, (a) 30% ultimate load (b) 50% ultimate load, (c) 80% ultimate load, (d) 100% ultimate load.*

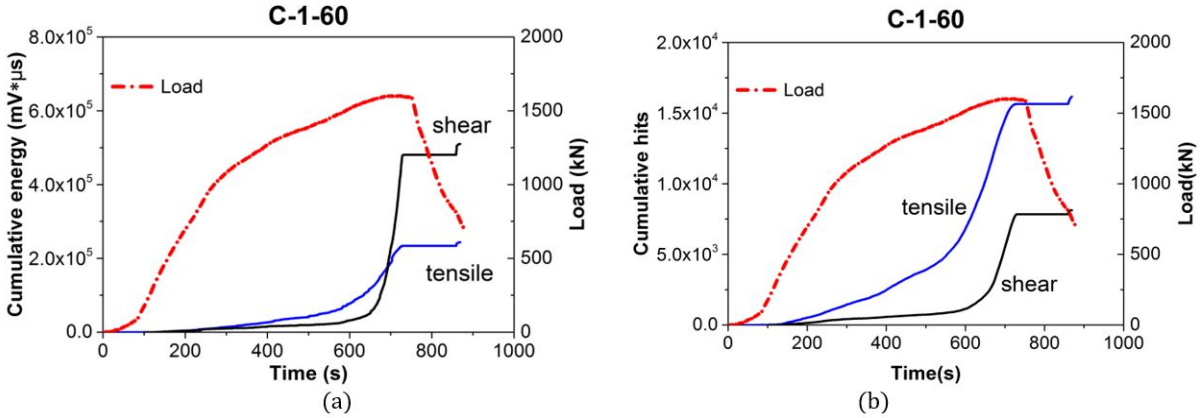

Figure 15: *AE progression of two crack clusters for C-1-60, (a) concrete cracking evolution versus cumulative AE energy, (b) concrete cracking evolution versus cumulative AE hits.*

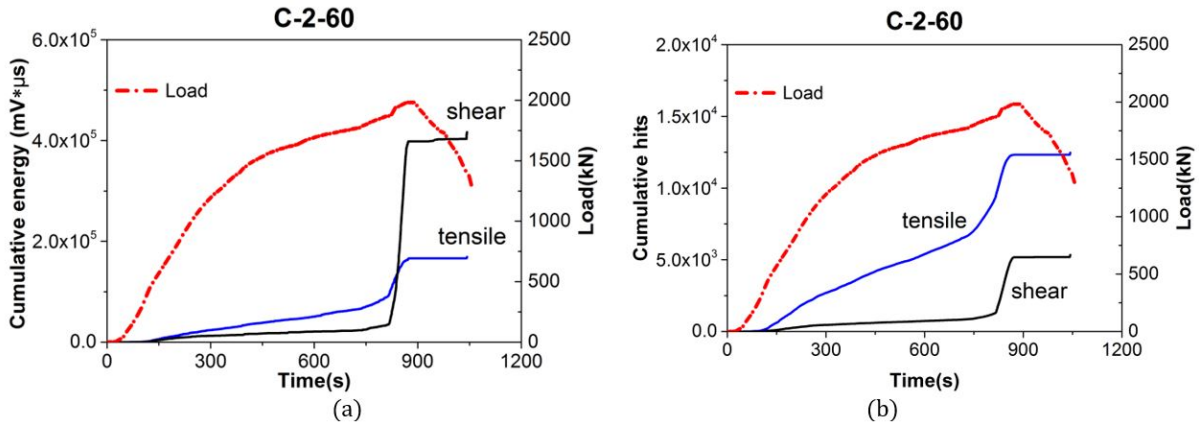

Figure 16: *AE progression of two crack clusters for C-2-60, (a) concrete cracking evolution versus cumulative AE energy, (b) concrete cracking evolution versus cumulative AE hits.*

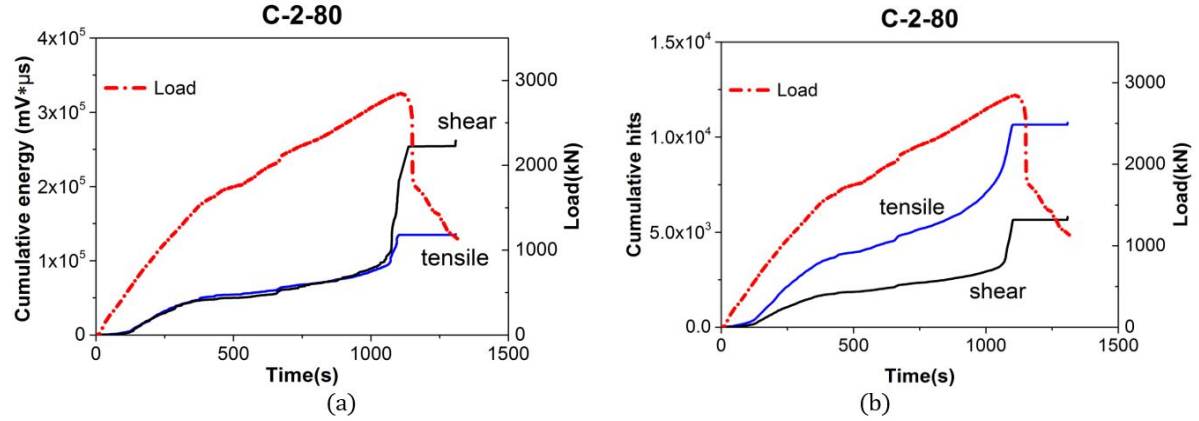

Figure 17: *AE progression of two crack clusters for C-2-80, (a) concrete cracking evolution versus cumulative AE energy, (b) concrete cracking evolution versus cumulative AE hits.*

6 CONCLUSIONS

AE technique is successfully applied to monitor the damage progression of the proposed STCRC columns under uniaxial compressive loading. The satisfactory monitoring and evaluating results provided preferably experimental evidence on the validity of AE technology as viable candidate tool for SHM and NDE for composite structures. Conclusions are drawn as follow:

The damage evolution of STCRC columns are investigated based on the variation of typical AE features, the proposed cumulative energy and AE rate provide quantitative information for damage severity, and the distinct knee point provide critical warning information before catastrophe.

The peak-frequency has proved to be a promising parameter to discriminate different damage modes, and the correlation analysis of AE energy and peak-frequency successfully disclosing the damage mechanisms for STCRC columns.

The concrete cracking modes are further analyzed based on RA value and average frequency, concrete cracks are automatically classified through the GMM algorithm from the perspective of uncertainty. Shear cracks cause less AE activity, however, contribute more to the final failure of STCRC columns.

ACKNOWLEDGMENTS

The authors are grateful for the financial support from the National Key Research and Development Program of China (Project No. 2017YFC0703410), and National Natural Science Foundation of China (NSFC) under Grant Nos. 51478079, 51778104.

References

Aggelis, D.G., (2011). Classification of cracking mode in concrete by acoustic emission parameters. Mechanics Research Communications 38(3): 153-157.

Ding, F.X., Yu, Z.W., Bai, Y., Gong, Y.Z., (2011). Elasto-plastic analysis of circular concrete-filled steel tube stub columns. Journal of Constructional Steel Research 67(10): 1567-1577.

Döhler, M., Hille, F., Mevel, L., Rücker, W., (2014). Structural health monitoring with statistical methods during progressive damage test of S101 Bridge. Engineering Structures 69(9): 183-193.

Du F., Li D., Shan B., Wang Y., (2018) Failure behavior monitoring and evaluation of steel-confined reinforced concrete columns by acoustic emission under quasi-static loading. Latin American Journal of Solids and Structures 15(11): e132.

Farhidzadeh, A., Dehghan-Niri, E., Salamone, S., Luna, B., Whittaker, A., (2013a). Monitoring Crack Propagation in Reinforced Concrete Shear Walls by Acoustic Emission. Journal of Structural Engineering 139(12): 116-134.

Farhidzadeh, A., Epackachi, S., Salamone, S., Whittaker, A.S., (2015). Bayesian decision and mixture models for AE monitoring of steel-concrete composite shear walls. Smart Materials and Structures 24(11): 115028.

Farhidzadeh, A., Salamone, S., Singla, P., (2013b). A probabilistic approach for damage identification and crack mode classification in reinforced concrete structures. Journal of Intelligent Material Systems and Structures 24(14): 1722-1735.

JCMS-III B5706 (2003). Monitoring method for active cracks in concrete by acoustic emission. Federation of Construction Materials Industries.

Liu, J., Zhang, S., Zhang, X., Guo, L., (2009). Behavior and strength of circular tube confined reinforced-concrete (CTRC) columns. Journal of Constructional Steel Research 65(7): 1447-1458.

Liu, X., Zhou, C., Jiang, Z., (2012). Damage localization in plate-like structure using built-in PZT sensor network. Smart Structures and Systems 9(1): 21-33.

Ma, G., Li, H., (2017). Acoustic emission monitoring and damage assessment of FRP-strengthened reinforced concrete columns under cyclic loading. Construction and Building Materials 144: 86-98.

Nair, A., Cai, C.S., (2010). Acoustic emission monitoring of bridges: Review and case studies. Engineering Structures 32(6): 1704-1714.

Ohno, K., Ohtsu, M., (2010). Crack classification in concrete based on acoustic emission. Construction and Building Materials 24(12): 2339-2346.

Philippidis, T.P., Assimakopoulou, T.T., (2008). Using acoustic emission to assess shear strength degradation in FRP composites due to constant and variable amplitude fatigue loading. Composites Science and Technology 68(3-4): 840-847.

Riyad, S.A., Rafael, M., (1998). Seismic resistance of steel confined reinforced concrete (SCRC) columns. Structural Design of Tall Buildings 7(3): 251-260.

Roberts, W., Furui, S., (2000). Maximum likelihood estimation of K-distribution parameters via the expectation-maximization algorithm. IEEE Transactions on Signal Processing 48(12): 3303-3306.

Sakino, K., Nakahara, H., Morino, S., Nishiyama, A., (2004). Behavior of centrally loaded concrete-filled steel-tube short columns. Jouranl of Structural Engineering 130(2): 180-188.

Schnabl, S., Planinc, I., (2017). Buckling of Slender Concrete-Filled Steel Tubes with Compliant Interfaces. Latin American Journal of Solids and Structures 14(10): 1837-1852.

Sengupta, S., Datta, A.K., Topdar, P., (2015). Structural damage localisation by acoustic emission technique: A state of the art review. Latin American Journal of Solids and Structures 12(8): 1565-1582.

Tagare, H.D., Barthel, A., Sigworth, F.J., (2010). An adaptive Expectation-Maximization algorithm with GPU implementation for electron cryomicroscopy. Journal of Structural Biology 171(3): 256-265.

Wang, Q., Ma, S., Yue, D., (2018). Identification of damage in composite structures using Gaussian mixture model-processed Lamb waves. Smart Materials and Structures, 27(4): 045007.

Wang, Y., Wang, W., Zhou, X., Liu, J., (2017). Experimental study on seismic behavior of steel tube confined reinforced concrete columns subjected to combined compression-bending-torsion. Journal of Building Structures 38(S1): 185-189.

Yang, C., Wu, Z., Zhang, Y., (2008). Structural health monitoring of an existing PC box girder bridge with distributed HCFRP sensors in a destructive test. Smart Materials and Structures 17(3): 035032.

Zhang, P., Sang, Y., Zhao, Z., Xu, Y., (2015). Application of Acoustic Emission Technique in Q345E Steel Tensile Damage Detection. Journal of Gansu Sciences 27(2): 83-87.

Zhou, X., Zhang, S., Liu, J., (2008). Seismic behavior of steel tube confined reinforced concrete (RC) beam-columns. Journal of Building Structures 29(5): 75-84.

Zitto, M.E., Piotrkowski, R., Gallego, A., Sagasta, F., Benavent-Climent, A., (2015). Damage assessed by wavelet scale bands and b-value in dynamical tests of a reinforced concrete slab monitored with acoustic emission. Mechanical Systems and Signal Processing 60-61: 75-89.